DALTON

Electrochemical deprotection of a substrate binding site in $[Mo_2(cp)_2(\mu\text{-}SMe)_3(\mu\text{-}Cl)]$ (cp = η^5-C_5H_5) *via* chloride-bridge opening. Kinetics of MeCN and Bu^{t}NC binding at this site†

Frédéric Barrière, Yves Le Mest, François Y. Pétillon, Sylvie Poder-Guillou, Philippe Schollhammer and Jean Talarmin *

URA CNRS 322 'Chimie, Electrochimie Moléculaires et Chimie Analytique', Département de Chimie, Université de Bretagne Occidentale, 6, Avenue V. Le Gorgeu, BP 809, 29285 Brest Cédex, France

The access to a co-ordination site in the quadruply bridged complex $[Mo_2(cp)_2(\mu\text{-}SMe)_3(\mu\text{-}Cl)]$ (cp = η^5-C_5H_5) has been found to be redox controlled. Electrochemical one-electron oxidation of the complex unlocks the chloride bridge but the radical cation retains the quadruply bridged geometry of the neutral parent as indicated by cyclic voltammetry and EPR spectroscopy. The chloride bridge opens up in the presence of a substrate (Y≡Z = MeCN, Bu^{t}NC, $Me_2C_6H_3NC$ or CO), leading to the formation of $[Mo_2(cp)_2(\mu\text{-}SMe)_3Cl(Y{\equiv}Z)]^{\bullet+}$ derivatives. The site is sensitive to the electronic properties of the substrate, and kinetic studies of the substrate-binding step demonstrated that Bu^{t}NC reacts faster and is bound more tightly at $[Mo_2(cp)_2(\mu\text{-}SMe)_3Cl]^{\bullet+}$ than is MeCN. The reduction of $[Mo_2(cp)_2(\mu\text{-}SMe)_3Cl(Y{\equiv}Z)]^{\bullet+}$ is reversible for Y≡Z = CO and RNC (R = Bu^t or $C_6H_3Me_2$) whereas MeCN is lost on reduction. In this case the fact that the chloride ligand is still present at the neighbouring molybdenum centre allows regeneration of the parent complex *via* bridge reclosure. The reactivity of $[Mo_2(cp)_2(\mu\text{-}SMe)_3(\mu\text{-}Cl)]$ in MeCN has also been investigated: instead of the bridge-opening process of the radical cation, the neutral parent loses the chloride bridge in MeCN; the resulting bis(acetonitrile) cation, $[Mo_2(cp)_2(\mu\text{-}SMe)_3(MeCN)_2]^+$, has been isolated and characterized.

The present report is a contribution to studies of electrochemically generated co-ordination sites. The exposure of a vacant site at a metal centre is a crucial step of catalytic processes either biological or industrial. In previous studies we observed that the sites, when generated in the absence of substrate, underwent a deactivation reaction leading to a stable species.[1,2] Such a reaction is undesirable since it competes with the formation of the site–substrate complex, particularly in the case of slow or reversible binding of the substrate. We have looked for different ways to suppress this unfavourable reaction,[2] and the work reported herein, which illustrates one of them, is concerned with the oxidative electrochemistry of $[Mo_2(cp)_2(\mu\text{-}SMe)_3(\mu\text{-}Cl)]$ (cp = η-C_5H_5). The electrochemistry of dimolybdenum complexes with halide bridge(s) is comparatively less well studied[3–5] than that of molybdenum (or other metal) complexes possessing terminal halide ligands, the electrochemical reduction of which can lead to the exposure of co-ordination sites.[1,6–9]

Here we show that the deprotection of the site, resulting from the opening of the chloride bridge of $[Mo_2(cp)_2(\mu\text{-}SMe)_3(\mu\text{-}Cl)]$, is redox-controlled, since substrates (Y≡Z) can bind only after one-electron oxidation of the complex; a characteristic of the process is that, if the complex $[Mo_2(cp)_2(\mu\text{-}SMe)_3Cl(Y{\equiv}Z)]^{\bullet+}$ releases the co-ordinated substrate, deactivation is prevented by the reformation of the original protective device. The work reported is concerned with a tris(thiolate)-bridged dimolybdenum compound, but the reactions described are reminiscent of redox-induced partial deco-ordination of chelating organic ligands[10–13] so one may consider that the site is generated at a $Mo(SMe)_3$ centre, a simple reactivity model of the molybdenum centre in the FeMo cofactor of nitrogenase.

† *Non-SI units employed:* atm = 101 325 Pa, G = 10^{-4} T.

Results and Discussion

Electrochemical studies

The cyclic voltammetry (CV) of $[Mo_2(cp)_2(\mu\text{-}SMe)_3(\mu\text{-}Cl)]$‡ in tetrahydrofuran (thf) and in CH_2Cl_2–$[NBu_4][PF_6]$ electrolytes shows two quasi-reversible, diffusion-controlled, one-electron oxidation steps $[(i_p^c/i_p^a)_{ox1} \approx 1, \Delta E_p = 90$ and 110 mV at a scan rate $v = 0.02$ and 0.2 V s^{-1}, respectively; $(i_p^c/i_p^a)_{ox2} < 1$, $\Delta E_p \approx 110$ mV at 0.2 V s^{-1}],§ Fig. 1(*a*), Table 1. The fact that the first oxidation process of the chloride-bridged complex is quasi-reversible in thf or CH_2Cl_2 electrolytes suggests that there is no major structural change coupled to the electron transfer, and that the radical cation retains the quadruply bridged structure of the neutral complex, Scheme 1. This is supported by EPR experiments (see below). Closely related quadruply bridged complexes such as $[Mo_2(cp)_2(\mu\text{-}SMe)_4]$[14] or $[Mo_2(cp)_2(\mu\text{-}X)_4]$ (X = Cl, Br or I)[4,5] also retain the structure of the parent on oxidation.

‡ The ^{1}H NMR spectrum of $[Mo_2(cp)_2(\mu\text{-}SMe)_3(\mu\text{-}Cl)]$ shows the presence of two isomers, which differ probably in the respective dispositions of the thiolate substituents. This might explain the slightly rounded shape of the first oxidation peak of the complex in thf–$[NBu_4][PF_6]$ [Fig. 1(*a*)]. This is not observed in CH_2Cl_2 or MeCN electrolytes, nor after one-electron oxidation [Fig. 1(*b*)]. The splitting of the more negative process of the $[Mo_2(cp)_2(\mu\text{-}SMe)_3Cl(Y{\equiv}Z)]^{0/\bullet+}$ complexes observed for Y≡Z = CO, Bu^{t}NC and 2,6-$Me_2C_6H_3NC$ in thf–$[NBu_4][PF_6]$ is also probably due to the presence of two isomers.

§ The parameters i_p^a and i_p^c are respectively the anodic and the cathodic peak currents of a reversible redox process, ΔE_p is the separation between these peaks; for a reversible one-electron system, ΔE_p is close to 60 mV. For the reversible oxidation of ferrocene, we find $\Delta E_p = 70$ (MeCN), 80 (CH_2Cl_2) and *ca.* 90–100 mV (thf); an EC process comprises an electron-transfer step (E) followed by a chemical reaction (C).

Table 1 Redox potentials (*vs.* ferrocene–ferrocenium) as measured by cyclic voltammetry[a]

Complex	Solvent	$E^{\ddagger}_{ox1}$/V	$E^{\ddagger}_{ox2}$/V
$[Mo_2(cp)_2(\mu\text{-}SMe)_3(\mu\text{-}Cl)]$	thf	−0.40	0.34
	CH_2Cl_2	−0.41	0.44
	MeCN	−0.40[b]	0.40(E_p)[b]
		−0.38 (−0.72)[c]	0.18
$[Mo_2(cp)_2(\mu\text{-}SMe)_3(MeCN)_2]^{+}$[d]	MeCN	−0.20	0.45
$[Mo_2(cp)_2(\mu\text{-}SMe)_3Cl(MeCN)]^{\cdot+}$	MeCN	−0.72 (−0.38)[c]	0.18
	thf	−0.77 (−0.36)[c]	0.14
$[Mo_2(cp)_2(\mu\text{-}SMe)_3Cl(CNBu^t)]^{\cdot+}$	thf	−0.64, −0.71	0.29
	CH_2Cl_2	−0.67	0.40
	MeCN	−0.67	0.35
$[Mo_2(cp)_2(\mu\text{-}SMe)_3Cl(CNC_6H_3Me_2)]^{\cdot+}$	thf	−0.61, −0.68	0.36
$[Mo_2(cp)_2(\mu\text{-}SMe)_3Cl(CO)]^{\cdot+}$	thf	−0.45, −0.51	0.77[e]

[a] $\nu = 0.2$ V s^{-1}, vitreous carbon electrode. [b] $\nu = 1$ V s^{-1}. [c] The reduction peak (−0.72 in MeCN, −0.77 V in thf) is irreversible and associated with an irreversible oxidation peak (−0.38 in MeCN, −0.36 V in thf). [d] Irreversible reduction at $E_{p,red} = -2.2$V. [e] Irreversible.

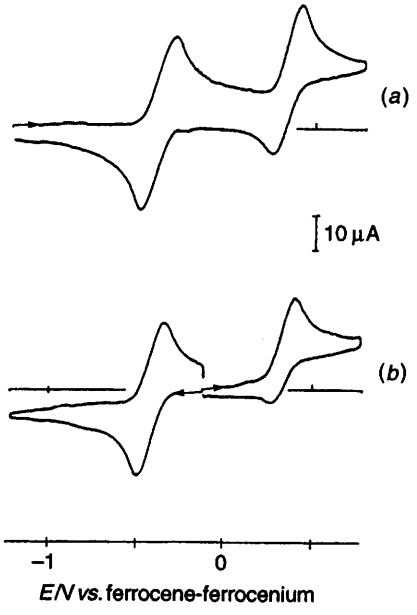

Fig. 1 Cyclic voltammetry of a 1.1 mmol dm^{-3} solution of $[Mo_2(cp)_2(\mu\text{-}SMe)_3(\mu\text{-}Cl)]$ in thf–$[NBu_4][PF_6]$ (*a*) before and (*b*) after controlled-potential oxidation at −0.1 V ($n = 0.97$ F mol^{-1} starting material). Scan rate 0.2 V s^{-1}, vitreous carbon electrode

Controlled-potential electrolysis (CPE) carried out at the potential of the first process converts the neutral complex into the corresponding radical cation after *ca.* 1 F mol^{-1} starting material has passed [Fig. 1(*b*)]. Addition of 1 equivalent HBF_4–Et_2O to a solution of $[Mo_2(cp)_2(\mu\text{-}SMe)_3(\mu\text{-}Cl)]$ in thf or in CH_2Cl_2 also results in a one-electron oxidation of the complex: CV of the oxidized solution shows the first step to be now a reduction.

Electron-transfer-induced opening of the chloride bridge in the presence of a substrate. In contrast with the results obtained in thf and CH_2Cl_2 electrolytes, the first oxidation of $[Mo_2(cp)_2(\mu\text{-}SMe)_3(\mu\text{-}Cl)]$ in MeCN–$[NBu_4][PF_6]$ shows some reversibility ($E^{\ddagger}_{ox1} = -0.40$ V) only for scan rates larger than *ca.* 0.4 V s^{-1}. At lower v this step is irreversible, with an oxidation–reduction peak separation of 0.34 V [Fig. 2(*a*),* Table 1]. This demonstrates that the oxidized complex, $[Mo_2(cp)_2(\mu\text{-}SMe)_3(\mu\text{-}Cl)]^{\cdot+}$, is involved in a fast chemical reaction. The EC process leads to a species having redox steps detected at 0.18 (reversible one-electron oxidation) and −0.72V (irreversible reduction), and which is obtained by controlled-potential

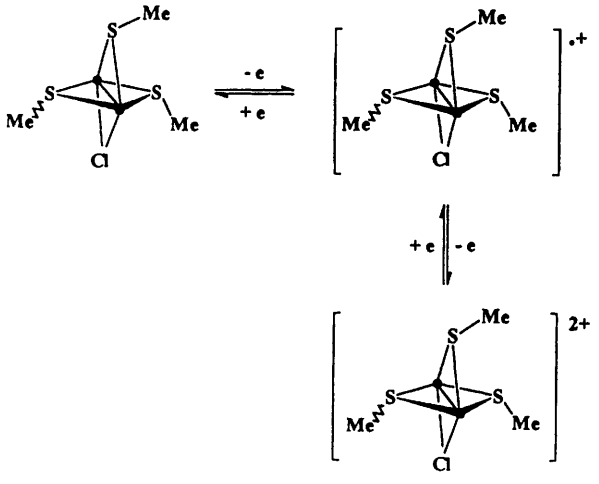

Scheme 1 ● = Mo(cp)

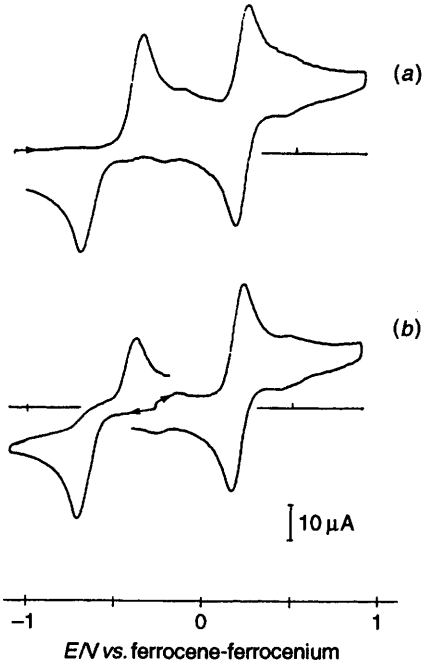

Fig. 2 Cyclic voltammetry of a 1.1 mmol dm^{-3} solution of $[Mo_2(cp)_2(\mu\text{-}SMe)_3(\mu\text{-}Cl)]$ in MeCN–$[NBu_4][PF_6]$ (*a*) before and (*b*) after controlled-potential oxidation at 0 V ($n = 0.87$ F mol^{-1} starting material). Scan rate 0.2 V s^{-1}, vitreous carbon electrode

* The small peaks around −0.2 and 0.45 V in Fig. 2 are due to the presence of some $[Mo_2(cp)_2(\mu\text{-}SMe)_3(MeCN)_2]^{+}$ (Table 1). This species, which arises from the reaction of $[Mo_2(cp)_2(\mu\text{-}SMe)_3(\mu\text{-}Cl)]$ in MeCN–$[NBu_4][PF_6]$ (see Fig. 10), is also observed after electrochemical reduction of $[Mo_2(cp)_2(\mu\text{-}SMe)_3Cl(MeCN)]^{\cdot+}$ in this electrolyte.

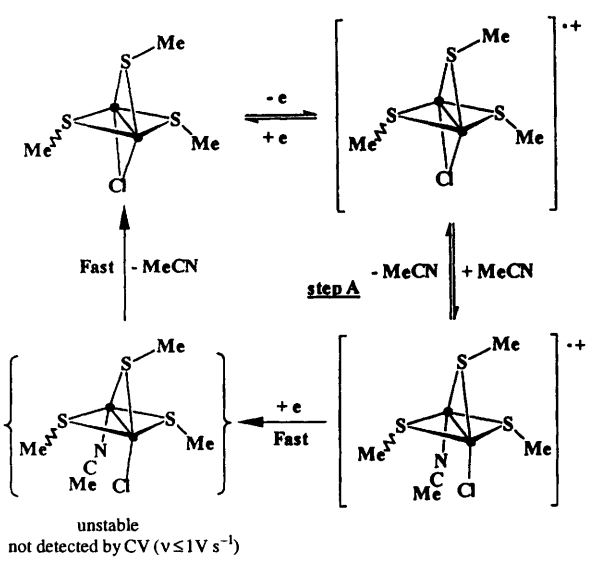

Scheme 2 ● = Mo(cp)

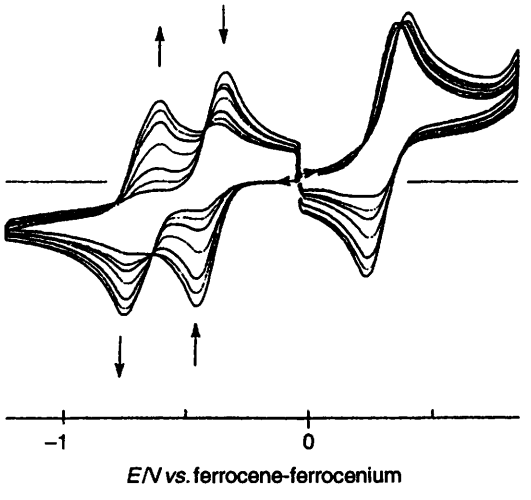

Fig. 3 Time dependence of the cyclic voltammetry of $[Mo_2(cp)_2(\mu\text{-}SMe)_3(\mu\text{-}Cl)]^{\bullet+}$ (3 mmol dm^{-3}) after addition of 1 equivalent Bu^tNC (thf–$[Bu_4N][PF_6]$; scan rate 0.2 V s^{-1}; vitreous carbon electrode)

oxidation, $n = 0.9 \pm 0.1$ F mol^{-1} initial complex [Fig. 2(*b*)]. The chemical step of the EC process is assigned as the opening of the chloride bridge, concerted with MeCN binding at the neighbouring Mo, Scheme 2. The binding of MeCN is supported by the fact that the first oxidation of $[Mo_2(cp)_2(\mu\text{-}SMe)_3(\mu\text{-}Cl)]$ becomes less reversible in thf and CH_2Cl_2 electrolytes in the presence of MeCN $[(i_p^c/i_p^a) < 1]$, and an irreversible reduction peak, due to the acetonitrile derivative, is then observed.

The electrochemical reduction of $[Mo_2(cp)_2(\mu\text{-}SMe)_3Cl(MeCN)]^{\bullet+}$ is irreversible and regenerates the initial chloride-bridged structure [Fig. 2(*b*), Scheme 2]. The kinetic experiments described below demonstrate that MeCN deco-ordination from $[Mo_2(cp)_2(\mu\text{-}SMe)_3Cl(MeCN)]^{\bullet+}$ can occur. It was therefore important to determine whether the reduction of this complex takes place according to a CE process (MeCN loss prior to electron transfer), or to an EC mechanism involving an undetected intermediate (electron-transfer-induced MeCN deco-ordination). Variable-scan-rate CV of $[Mo_2(cp)_2(\mu\text{-}SMe)_3Cl(MeCN)]^{\bullet+}$ shows that at low v the reduction peak of the complex shifts cathodically by *ca.* 30 mV for a ten-fold increase in v (from 0.02 to 0.2 V s^{-1}); at faster scan rates this shift is less important, with a cathodic shift of *ca.* 20 mV for CV run at 0.1 and at 1 V s^{-1}. For $0.1 \leqslant v \leqslant 1$ V s^{-1} the current function $i_{p,red}/v^{\frac{1}{2}}$ is almost independent of v, although it

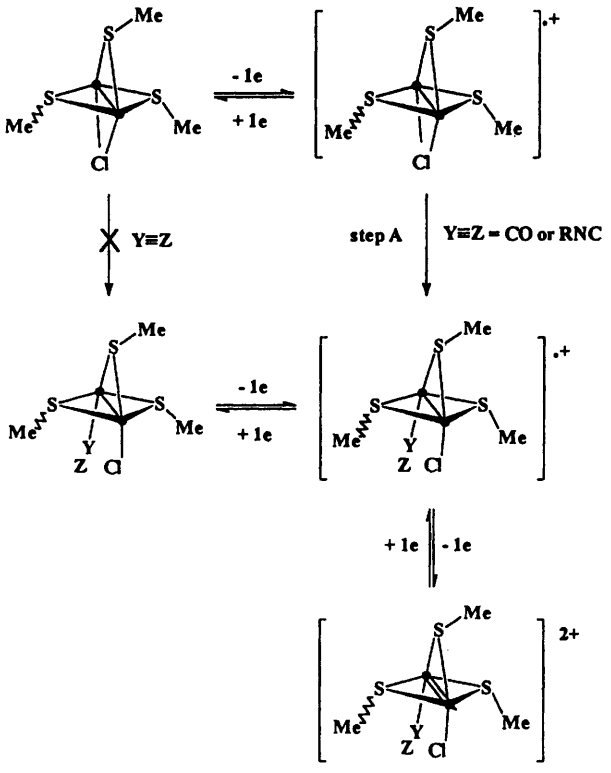

Scheme 3 ● = Mo(cp), R = Bu^t or $C_6H_3Me_2$

decreases slightly with decreasing scan rates for $0.02 \leqslant v < 0.1$ V s^{-1}. These data suggest that an irreversible chemical reaction is coupled after the electron transfer step (EC_{irr} process[15]). From these experiments it can be concluded that electron transfer to $[Mo_2(cp)_2(\mu\text{-}SMe)_3Cl(MeCN)]^{\bullet+}$ is faster than deco-ordination of MeCN from it. The chemical step of the EC_{irr} process is fast: the undetected ($v \leqslant 1$ V s^{-1}) $[Mo_2(cp)_2(\mu\text{-}SMe)_3Cl(MeCN)]$ intermediate loses the MeCN ligand very rapidly (Scheme 2).

The electron-transfer-induced opening of the chloride bridge observed in the MeCN electrolyte led us to investigate the electrochemical behaviour of $[Mo_2(cp)_2(\mu\text{-}SMe)_3(\mu\text{-}Cl)]$ in the presence of various substrates, in thf–$[NBu_4][PF_6]$. Although the cyclic voltammetry ($v = 0.2$ V s^{-1}) of $[Mo_2(cp)_2(\mu\text{-}SMe)_3(\mu\text{-}Cl)]$ in thf–$[NBu_4][PF_6]$ is not affected by the presence of isocyanide (1–3 equivalents Bu^tNC), controlled-potential oxidation performed under these conditions at the potential of the first process leads to the formation of $[Mo_2(cp)_2(\mu\text{-}SMe)_3(Cl)(Bu^tNC)]^{\bullet+}$, after the passage of 0.9 ± 0.1 F mol^{-1} starting material. The isocyanide derivative was identified by comparing its redox potentials (Table 1) with those of a sample of this complex prepared by chemical oxidation of $[Mo_2(cp)_2(\mu\text{-}SMe)_3(\mu\text{-}Cl)]$ in the presence of Bu^tNC and characterized by microanalyses. Monitoring by CV of the reaction of $[Mo_2(cp)_2(\mu\text{-}SMe)_3(\mu\text{-}Cl)]^{\bullet+}$ with 1 equivalent Bu^tNC is shown in Fig. 3: the presence of iso-potential points[16] on the curves demonstrates the absence of side reactions, confirmed by the almost quantitative formation of the isocyanide complex (> 85%) the redox steps of which are detected by CV (Scheme 3). The yield was calculated from a comparison of the reduction peak current of the reactant $[Mo_2(cp)_2(\mu\text{-}SMe)_3(\mu\text{-}Cl)]^{\bullet+}$ with the oxidation peak current of the product $[Mo_2(cp)_2(\mu\text{-}SMe)_3Cl(Bu^tNC)]^{\bullet+}$, assuming identical diffusion coefficients for both species.

Controlled-potential reduction of $[Mo_2(cp)_2(\mu\text{-}SMe)_3Cl(Bu^tNC)]^{\bullet+}$ ($n = 0.8 \pm 0.1$ F mol^{-1} of the parent) affords the neutral derivative (*ca.* 80–85%, CV measurement), which is not accessible directly from $[Mo_2(cp)_2(\mu\text{-}SMe)_3(\mu\text{-}Cl)]$ and Bu^tNC under our experimental conditions (Scheme 3). A close inspection of the reduction peak of $[Mo_2(cp)_2(\mu$-

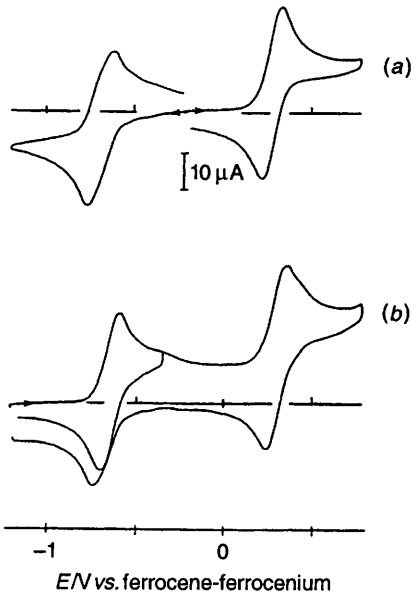

Fig. 4 Cyclic voltammetry (*a*) of a 3 mmol dm^{-3} solution of $[Mo_2(cp)_2(\mu\text{-}SMe)_3(\mu\text{-}Cl)]$ after controlled-potential oxidation at −0.1 V (0.9 F mol^{-1}) in the presence of 1 equivalent Bu^{t}NC, (*b*) the same solution after reduction at −1.1 V (0.85 F mol^{-1}) (thf–$[Bu_4N][PF_6]$; scan rate 0.2 V s^{-1}; vitreous carbon electrode)

$SMe)_3Cl(Bu^tNC)]^{\bullet+}$ [Fig. 4(*a*)] shows it comprises two overlapping redox processes. This suggests that the radical cation exists as a mixture of two isomers the reduction potentials of which are similar in thf–$[NBu_4][PF_6]$ (and unresolved in MeCN and CH_2Cl_2 electrolytes, Table 1) and which oxidize at the same potential of 0.29V. The nature of the isomerism is not known, but a difference in the orientation of the sulfur substituents (axial *vs.* equatorial) is a possibility. On the contrary, CV of $[Mo_2(cp)_2(\mu\text{-}SMe)_3Cl(Bu^tNC)]$ shows two reversible one-electron oxidation steps, with no splitting of the first [Fig. 4(*b*)]. Similar phenomena are observed with $Me_2C_6H_3NC$ except that the overlapping redox processes are observed in the CV of $[Mo_2(cp)_2(\mu\text{-}SMe)_3Cl(Me_2C_6H_3NC)]$ rather than in that of the corresponding radical cation.

Reactions of CO and CN^- with $[Mo_2(cp)_2(\mu\text{-}SMe)_3(\mu\text{-}Cl)]^{\bullet+}$ have also been investigated in thf–$[NBu_4][PF_6]$. The addition of 1 equivalent $[NBu_4][CN]$ to a solution of the radical cation causes instant reduction to the neutral complex, whereas controlled-potential oxidation of $[Mo_2(cp)_2(\mu\text{-}SMe)_3(\mu\text{-}Cl)]$ under 1 atm CO produces a mixture of $[Mo_2(cp)_2(\mu\text{-}SMe)_3(\mu\text{-}Cl)]^{\bullet+}$ and $[Mo_2(cp)_2(\mu\text{-}SMe)_3Cl(CO)]^{\bullet+}$. This is due to a slow reaction of CO with $[Mo_2(cp)_2(\mu\text{-}SMe)_3(\mu\text{-}Cl)]^{\bullet+}$ on the CPE time-scale rather than to an equilibrium, as shown by CV monitoring of a solution of $[Mo_2(cp)_2(\mu\text{-}SMe)_3(\mu\text{-}Cl)]^{\bullet+}$ under 1 atm CO, and by the fact that the carbonyl derivative is obtained almost quantitatively for longer reaction times (Experimental section).

The redox potentials of the $[Mo_2(cp)_2(\mu\text{-}SMe)_3Cl(Y{\equiv}Z)]^{\bullet+}$ complexes are sensitive to the nature of the Y≡Z ligand (Table 1). Plots of the $E^{\frac{1}{2}}$ potentials *vs.* the P_L values[17] of the different ligands* are linear, with the slope (1.09) of the line for the oxidation potentials being more than twice that (0.45) for the reduction potentials (Fig. 5). Therefore, the difference between the oxidation and the reduction steps of $[Mo_2(cp)_2(\mu\text{-}SMe)_3Cl(Y{\equiv}Z)]^{\bullet+}$ is sensitive to the variations of the σ-donor/π-acceptor properties of the different ligands. These results show that the highest occupied molecular orbital (HOMO) of $[Mo_2(cp)_2(\mu\text{-}SMe)_3Cl(Y{\equiv}Z)]$ receives a contribution from Y≡Z orbitals. In addition, if the presence of Mo–Mo bond(s) is not taken into account, the metal centres in $[Mo_2(cp)_2(\mu\text{-}SMe)_3Cl(Y{\equiv}Z)]^n$ possess a 16- ($n = +2$) or a 17-electron ($n = 0$) count so that a metal–metal double and a single bond are expected in these compounds, respectively, for the metal centres to reach the closed-shell configuration. The two-electron oxidation of $[Mo_2(cp)_2(\mu\text{-}SMe)_3Cl(Y{\equiv}Z)]$ would therefore lead to the formation of a metal–metal bond, which indicates that the HOMO should also have a Mo–Mo antibonding character.

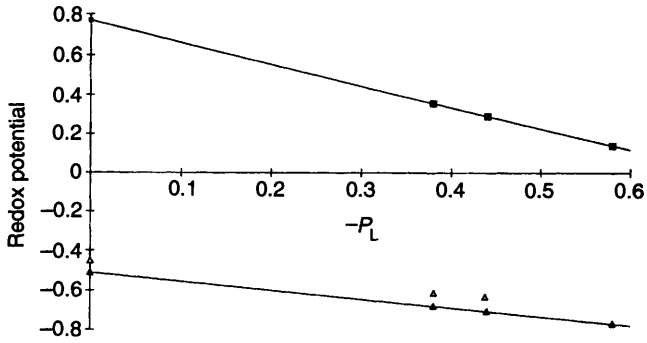

Fig. 5 Plots of the redox potentials of $[Mo_2(cp)_2(\mu\text{-}SMe)_3Cl(Y{\equiv}Z)]^{\bullet+}$ *vs.* the ligand parameter[17] P_L. The potentials measured for both isomers of the complexes where Y≡Z = CO, $Me_2C_6H_3NC$ and Bu^{t}NC are indicated

Fig. 6 The EPR spectrum of $[Mo_2(cp)_2(\mu\text{-}SMe)_3(\mu\text{-}Cl)]^{\bullet+}$ in CH_2Cl_2 at −50 °C showing part of the six- and 11-line patterns. Insert: EPR spectrum of $[Mo_2(cp)_2(\mu\text{-}SMe)_4]^{\bullet+}$ in CH_2Cl_2 at −50 °C

EPR studies

The EPR parameters of the complexes are listed in Table 2. The spectra of $[Mo_2(cp)_2(\mu\text{-}SMe)_3(\mu\text{-}Cl)]^{\bullet+}$ prepared either electrochemically or by HBF_4–Et_2O oxidation in CH_2Cl_2 are identical. At *ca.* −50 °C in CH_2Cl_2 they show hyperfine coupling consistent with delocalization of the unpaired electron over two equivalent molybdenum nuclei (Class III complex[21]). The spectra consist of an intense central signal due to the dimer with $I_{Mo1} = I_{Mo2} = 0$. Hyperfine coupling for the less-abundant dimers with $I_{Mo1} = 0$ and $I_{Mo2} = \frac{5}{2}$ and with $I_{Mo1} = I_{Mo2} = \frac{5}{2}$, gives rise to a lower-intensity sextet and to a very low-intensity 11-line pattern, respectively. Four lines of the sextet and three of the 11-line spectrum are shown in Fig. 6. This spectrum is very similar to that of $[Mo_2(cp)_2(\mu\text{-}SMe)_4)]^{\bullet+}$ recorded under the same conditions (Fig. 6, insert). The hyperfine coupling with both molybdenum nuclei is consistent with the HOMO of the μ-Cl complex being a Mo–Mo δ orbital, as it has been calculated for the $[Mo_2(cp)_2(\mu\text{-}Cl)_4)]$[22] and $[Mo_2(cp)_2(\mu\text{-}SH)_4]$[23,24] analogues.

The EPR spectra of $[Mo_2(cp)_2(\mu\text{-}SMe)_3Cl(Y{\equiv}Z)]^{\bullet+}$ with Y≡Z = CO, Bu^{t}NC, $Me_2C_6H_3NC$ or MeCN are all similar. They consist of a central line with a lower-intensity sextet (Fig. 7, Y≡Z = MeCN); the intensity of the sextet relative to that of the central signal is indicative of a Class I[21] complex with the

* L = CO, $P_L = 0$;[17] MeCN, −0.58;[17] Bu^{t}NC, −0.44;[18] for $Me_2C_6H_3NC$ we have used the same P_L value as for PhNC, −0.38.[17]

Table 2 The EPR spectral data in CH_2Cl_2

Complex	T/°C	g	A_{Mo}/G
$[Mo_2(cp)_2(\mu\text{-}SMe)_3(\mu\text{-}Cl)]^{\bullet+}$	−50	2.000	19.3
$[Mo_2(cp)_2(\mu\text{-}SMe)_4]^{\bullet+}$	−50	2.011	18
	−60[a]	2.007[a]	18[a]
	r.t.[b]	2.009[b]	—
		2.027[c]	—
$[Mo_2(cp)_2(\mu\text{-}SMe)_3Cl(NCMe)]^{\bullet+}$	r.t.	2.015	33.8
$[Mo_2(cp)_2(\mu\text{-}SMe)_3Cl(CNBu^t)]^{\bullet+}$	r.t.	2.015	36.6
$[Mo_2(cp)_2(\mu\text{-}SMe)_3Cl(CNC_6H_3Me_2)]^{\bullet+}$	r.t.	2.012	34.8
$[Mo_2(cp)_2(\mu\text{-}SMe)_3Cl(CO)]^{\bullet+}$	r.t.	2.017	35.2

r.t. = Room temperature. [a] Ref. 19. [b] Ref. 14. [c] Ref. 20.

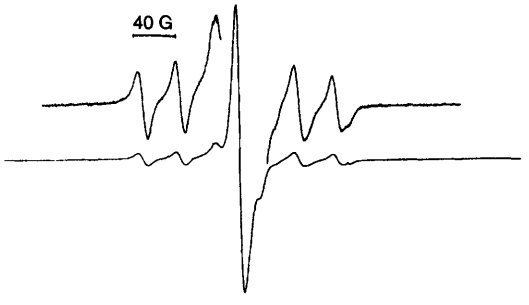

Fig. 7 The EPR spectrum of $[Mo_2(cp)_2(\mu\text{-}SMe)_3Cl(MeCN)]^{\bullet+}$ in MeCN at room temperature

unpaired electron localized on one molybdenum centre. This is in agreement with the values of the coupling constants (A_{Mo}, Table 2), which are approximately twice that of $[Mo_2(cp)_2(\mu\text{-}SMe)_3(\mu\text{-}Cl)]^{\bullet+}$. Hyperfine coupling of the unpaired electron with only one molybdenum nucleus and the absence of hyperfine coupling with chloride suggest that the unpaired electron is localized on the Mo(Y≡Z) centre. A quite different situation is observed when $[Mo_2(cp)_2(\mu\text{-}SMe)_3(\mu\text{-}Cl)]^{\bullet+}$ is treated with anionic species (NO_3^-, ClO_4^-). The EPR spectra show hyperfine coupling with one Mo ($A_{Mo} \approx 37$ G) and superhyperfine coupling with the chloride ligand ($I = \frac{3}{2}$, $A_{Cl} \approx 3$ G), indicating that the unpaired electron resides in an orbital with Mo–Cl character.[25]

If the HOMO of $[Mo_2(cp)_2(\mu\text{-}SMe)_3(\mu\text{-}Cl)]$ is a δ orbital one does not expect oxidation to affect the stability of the chloride bridge of the radical cation. The EPR results confirm that $[Mo_2(cp)_2(\mu\text{-}SMe)_3(\mu\text{-}Cl)]^{\bullet+}$ retains the quadruply bridged geometry of the neutral parent in the absence of a potential ligand, since hyperfine coupling with two equivalent molybdenum nuclei is observed. Nevertheless, the chloride bridge of the radical cation opens up in the presence of a substrate * whereas this process does not take place for the neutral complex. Therefore, the one-electron oxidation of the neutral parent unlocks the access to the co-ordination site (tantamount to saying that the increased electrophilicity of the radical cation favours co-ordination of the Y≡Z nucleophile *via* chloride-bridge opening). A similar process has been reported in the case of $[Mo_2(cp)_2(\mu\text{-}Cl)_4]^{\bullet+}$ which produces $[Mo_2(cp)_2(\mu\text{-}Cl)_3Cl_2]$ in the presence of chloride.[4] Theoretical calculations[26] of the electronic structure of $[Mo_2(cp)_2(\mu\text{-}Cl)_3Cl_2]^+$ demonstrate the same orbital ordering as for $[Mo_2(cp)_2(\mu\text{-}Cl)_4]$[22] (*e.g.* σδ*δ), so both $[Mo_2(cp)_2(\mu\text{-}Cl)_4]^{\bullet+}$ and $[Mo_2(cp)_2(\mu\text{-}Cl)_3Cl_2]$ have the $\sigma^2\delta^{*2}\delta^1$ electronic configuration. In the case of our complexes, EPR and electrochemical data suggest that the unpaired

* It is worth mentioning that this is not observed for $[Mo_2(cp)_2(\mu\text{-}SMe)_4]^{\bullet+}$ which can be prepared by controlled-potential oxidation of the neutral parent in MeCN–$[NBu_4][PF_6]$. For $[Mo_2(cp)_2(\mu\text{-}SMe)_4]^{\bullet+}$, $E^{\frac{1}{2}}_{red} = -0.53$ V and $E^{\frac{1}{2}}_{ox} = 0.26$ V in MeCN–$[NBu_4][PF_6]$.

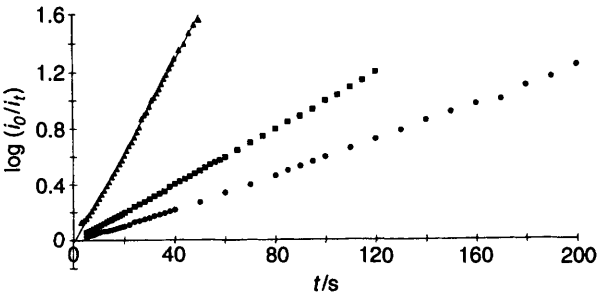

Fig. 8 Plots of log (i_0/i_t) *vs.* time obtained during the reaction of $[Mo_2(cp)_2(\mu\text{-}SMe)_3(\mu\text{-}Cl)]^{\bullet+}$ (1.1 mmol dm^{-3}) with Bu^tNC [2.4 × 10^{-2} (●), 3.9 × 10^{-2} (■) or 1.24 × 10^{-1} mol dm^{-3} (▲)] at room temperature in thf–$[NBu_4][PF_6]$. Amperometry at a rotating (5000 revolutions min^{-1}) vitreous carbon disc electrode; potential −0.5 V

electron resides in an orbital which has a different composition for $[Mo_2(cp)_2(\mu\text{-}SMe)_3(\mu\text{-}Cl)]^{\bullet+}$ and for $[Mo_2(cp)_2(\mu\text{-}SMe)_3Cl(Y{\equiv}Z)]^{\bullet+}$. In the absence of MO calculations on these complexes one can assume that the opening of the chloride bridge of the radical cation concerted with the co-ordination of Y≡Z lowers the total energy of the system.

Reactivity of $[Mo_2(cp)_2(\mu\text{-}SMe)_3Cl]^{\bullet+}$ in the presence of cosubstrates, Bu^tNC and MeCN

The selectivity of the $[Mo_2(cp)_2(\mu\text{-}SMe)_3Cl]^{\bullet+}$ co-ordination site is revealed in different ways. First, among the substrates we have studied, cyanide ion is not durably bound at the site which is reduced to the parent neutral complex. Secondly, CO reacts with the site more slowly than do Bu^tNC and MeCN. Thirdly, MeCN, which binds to $[Mo_2(cp)_2(\mu\text{-}SMe)_3(\mu\text{-}Cl)]^{\bullet+}$, is lost on reduction. This suggests how the reduction of a substrate at a given metal centre could be inhibited by a species not reducible at the same centre. In the present case, MeCN, which could not possibly be reduced at the $[Mo_2(cp)_2(\mu\text{-}SMe)_3Cl]^{\bullet+}$ site since the reduction of $[Mo_2(cp)_2(\mu\text{-}SMe)_3Cl(MeCN)]^{\bullet+}$ regenerates the parent chloride-bridged complex (see above), could inhibit the binding (and a possible subsequent reduction) of Bu^tNC, provided the rates of the reaction of MeCN and Bu^tNC with the site were similar.

Controlled-potential electrolyses of $[Mo_2(cp)_2(\mu\text{-}SMe)_3(\mu\text{-}Cl)]$ performed in MeCN–$[NBu_4][PF_6]$ in the presence of Bu^tNC (2, 10, 20 equivalents) lead to a mixture of the MeCN- and Bu^tNC-containing radical cations. While this mixture is stirred under N_2 the redox systems of the isocyanide derivative increase at the expense of those of the acetonitrile analogue. In thf, however, MeCN does not compete efficiently with isocyanide for the $[Mo_2(cp)_2(\mu\text{-}SMe)_3Cl]^{\bullet+}$ site. Controlled-potential electrolysis of $[Mo_2(cp)_2(\mu\text{-}SMe)_3(\mu\text{-}Cl)]$ carried out in thf–$[NBu_4][PF_6]$ in the presence of equivalent amounts of Bu^tNC and MeCN (3 equivalents each) produces only the isocyanide derivative.

We have undertaken a kinetic study of the co-ordination step of MeCN and Bu^tNC in order to rationalize these observations.

Kinetic analysis of the substrate-binding step

As the unsubstituted radical cation reduces at a potential less negative than those of the acetonitrile or isocyanide derivatives, the rate of substrate binding (step A in Schemes 2 and 3) can be readily monitored by amperometry at a rotating-disc electrode set at −0.5 V. Kinetic analyses were performed under pseudo-first-order conditions in thf–$[NBu_4][PF_6]$, with Y≡Z = Bu^tNC or MeCN. When Y≡Z = Bu^tNC, plots of (log i_0/i_t) *vs.* time are linear (i_0 and i_t are the initial current and the current at instant t, respectively), and an apparent rate constant can be calculated. As shown in Fig. 8, the slopes of the lines depend on the initial substrate concentration. The pseudo-first-order rate constants obtained from the amperometric studies were plotted against

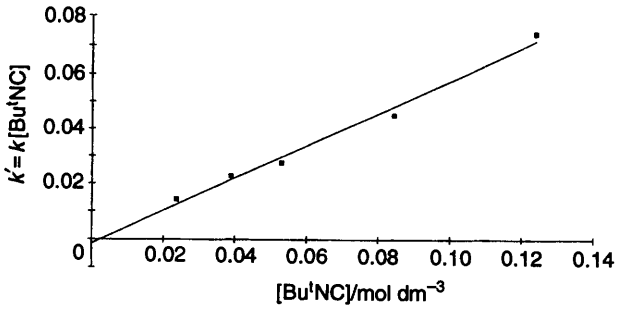

Fig. 9 Plot of k' *vs.* Bu^{t}NC concentration obtained for the reaction of $[Mo_2(cp)_2(\mu\text{-}SMe)_3(\mu\text{-}Cl)]^{\bullet+}$ with Bu^{t}NC at room temperature in thf–$[NBu_4][PF_6]$

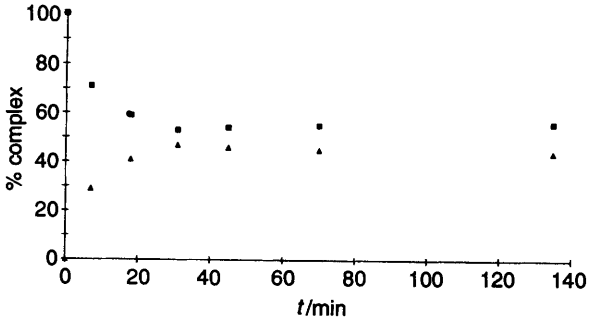

Fig. 10 Time dependence of the distribution of $[Mo_2(cp)_2(\mu\text{-}SMe)_3(\mu\text{-}Cl)]$ (■) and $[Mo_2(cp)_2(\mu\text{-}SMe)_3(MeCN)_2]^+$ (▲) in MeCN–$[NBu_4][PF_6]$

five different initial isocyanide concentrations in order to determine the second-order rate constant for substrate binding, at room temperature. This is shown in Fig. 9 from which the rate constant k was calculated, as $(5.9 \pm 0.3) \times 10^{-1}$ dm^3 mol^{-1} s^{-1}.

Amperometric monitoring of the reaction of $[Mo_2(cp)_2(\mu\text{-}SMe)_3(\mu\text{-}Cl)]^{\bullet+}$ with MeCN showed a quite different behaviour from that described above. After an initial decay of the current an equilibrium is reached; this is in agreement with the results of CPE carried out in acetonitrile in the presence of Bu^{t}NC. The kinetics of the forward and reverse reactions of step A (Scheme 2) were analysed in two different situations, that is for solutions containing initially $[Mo_2(cp)_2(\mu\text{-}SMe)_3(\mu\text{-}Cl)]^{\bullet+}$ as the only metal complex and for those containing both $[Mo_2(cp)_2(\mu\text{-}SMe)_3(\mu\text{-}Cl)]^{\bullet+}$ and $[Mo_2(cp)_2(\mu\text{-}SMe)_3Cl(MeCN)]^{\bullet+}$; the latter were obtained by successive additions of MeCN to a solution of the μ-chloro radical cation. The linear variations of $\log (i_0 - i_{eq})/(i_t - i_{eq})$ against time (see Experimental section) allowed the rate constant of the backward reaction to be calculated, $k_b = (3.8 \pm 0.5) \times 10^{-2}$ s^{-1}. The pseudo-first-order rate constant of the forward reaction was then obtained from the equation between k'_f, k_b and the equilibrium concentrations of reactant and product (see Experimental section), and the values of k'_f were plotted *vs.* several initial MeCN concentrations. The second-order rate constant for the direct reaction is $k_f = (2.4 \pm 0.3) \times 10^{-1}$ dm^3 mol^{-1} s^{-1}.

The kinetic studies reveal that, although the rates of the direct reactions of MeCN and Bu^{t}NC with the site are different, the main difference between these substrates lies with the reversibility of MeCN binding. This illustrates that MeCN is a weaker ligand than Bu^{t}NC for $[Mo_2(cp)_2(\mu\text{-}SMe)_3Cl]^{\bullet+}$ as well as it is a much poorer ligand than the isocyanide for the reduced site.

As mentioned above (Scheme 3), $[Mo_2(cp)_2(\mu\text{-}SMe)_3(\mu\text{-}Cl)]$ does not react with CO or Bu^{t}NC (1–5 equivalents) at room temperature on the time-scale of the electrochemical experiments in thf–$[NBu_4][PF_6]$, although the neutral carbonyl and isocyanide derivatives $[Mo_2(cp)_2(\mu\text{-}SMe)_3Cl(Y{\equiv}Z)]$ are stable complexes. Their formation from the μ-Cl complex requires an oxidation step to unlock the access to the co-ordination site, and then a reduction. In MeCN electrolyte, however, a reaction of the neutral chloride-bridged complex is observed.

Reaction of $[Mo_2(cp)_2(\mu\text{-}SMe)_3(\mu\text{-}Cl)]$ with MeCN: formation of $[Mo_2(cp)_2(\mu\text{-}SMe)_3(MeCN)_2]^+$

Monitoring by CV of a MeCN–$[NBu_4][PF_6]$ solution of $[Mo_2(cp)_2(\mu\text{-}SMe)_3(\mu\text{-}Cl)]$ demonstrates that this complex undergoes modification on standing. The product, showing two reversible one-electron oxidation processes and an irreversible reduction (Table 1), has been characterized as $[Mo_2(cp)_2(\mu\text{-}SMe)_3(MeCN)_2]^+$ from spectroscopic data (^{1}H NMR and infrared) and microanalysis (see Experimental section). Fig. 10 illustrates the decay of $[Mo_2(cp)_2(\mu\text{-}SMe)_3(\mu\text{-}Cl)]$ and the formation of the bis(acetonitrile) cation as measured from the ratio of the intensities of their first oxidation peak current; the equilibrium mixture contains these complexes in a *ca.* 55:45 ratio, respectively.

The formation of $[Mo_2(cp)_2(\mu\text{-}SMe)_3(MeCN)_2]^+$ is favoured by the addition of protons or of K^+: CV of a solution of $[Mo_2(cp)_2(\mu\text{-}SMe)_3(\mu\text{-}Cl)]$ in MeCN–$[NBu_4][PF_6]$ in the presence of 1 equivalent toluene-*p*-sulfonic acid or $HClO_4$, or in MeCN–KPF_6, demonstrates that the transformation of the chloride-bridged complex is much faster and complete under these conditions. Conversely, the formation of $[Mo_2(cp)_2(\mu\text{-}SMe)_3(MeCN)_2]^+$ is suppressed in the presence of chloride ($[NEt_4]Cl$), and the bis(acetonitrile) cation regenerates $[Mo_2(cp)_2(\mu\text{-}SMe)_3(\mu\text{-}Cl)]$ substantially in the presence of an excess (*ca.* 3 equivalents) Cl^-. The formation of $[Mo_2(cp)_2(\mu\text{-}SMe)_3(MeCN)_2]^+$ is not likely to proceed *via* $[Mo_2(cp)_2(\mu\text{-}SMe)_3Cl(MeCN)]$ since the electrochemical study described above demonstrates that this intermediate would undergo loss of MeCN rather than Cl^- (Scheme 2).

The effect of the solvent on the reaction of $[Mo_2(cp)_2(\mu\text{-}SMe)_3(\mu\text{-}Cl)]$ with protons is striking: this reaction, carried out in CH_2Cl_2 or in thf, leads to one-electron oxidation of the complex; this was used for the chemical syntheses of the μ-Cl radical cation and of its carbonyl and isocyanide derivatives in CH_2Cl_2. The formation of radical cations in these solvents indicates that the HOMO of the neutral parent is the site of proton attack, and therefore the reaction is orbitally controlled. If such were also the case in MeCN, $[Mo_2(cp)_2(\mu\text{-}SMe)_3Cl(MeCN)]^{\bullet+}$ should be produced on addition of H^+. However, the radical cation is not formed, and the only complexes detected during the course of the reaction are the μ-chloro parent and the final product. A difference in the oxidation potentials of complexes can be the reason for a different mode of control of the electrophilic reaction (orbital *vs.* charge control). We reported that this is why $[Mo_2(cp)_2(\mu\text{-}SR)_2(CO)(CN)]^-$ undergoes attack by Me_3O^+ at a sulfur lone pair when R = Me and at the cyanide ligand when R = CF_3.[27] Whether dinitrogen complexes are protonated or oxidized by protons was shown to depend on their oxidation potentials.[17,28] It has also been demonstrated that a 110 mV difference in the oxidation potentials of related bis(1,1-dithiolate)-bridged complexes is enough to switch the reaction with H^+ from a one-electron oxidation to a C–S bond cleavage.[29] However, $[Mo_2(cp)_2(\mu\text{-}SMe)_3(\mu\text{-}Cl)]$ oxidizes at the same potential in thf and in MeCN electrolytes (Table 1); it is therefore unlikely that the reaction in MeCN be under charge control, which might have explained proton attack at the chloride ligand. The fact that the reaction is under the same control in both solvents should produce the same effects (one-electron oxidation), unless a different species is present in MeCN: we propose that the chloride-bridged complex equilibrates with a solvent-separated ion pair (due to the dissociating nature of the MeCN solvent, Scheme 4, step a), which would react readily with the solvent (step b). In the absence of H^+ (or K^+) an equilibrium is reached since $[Mo_2(cp)_2(\mu\text{-}SMe)_3(MeCN)_2]^+$ reacts with Cl^-

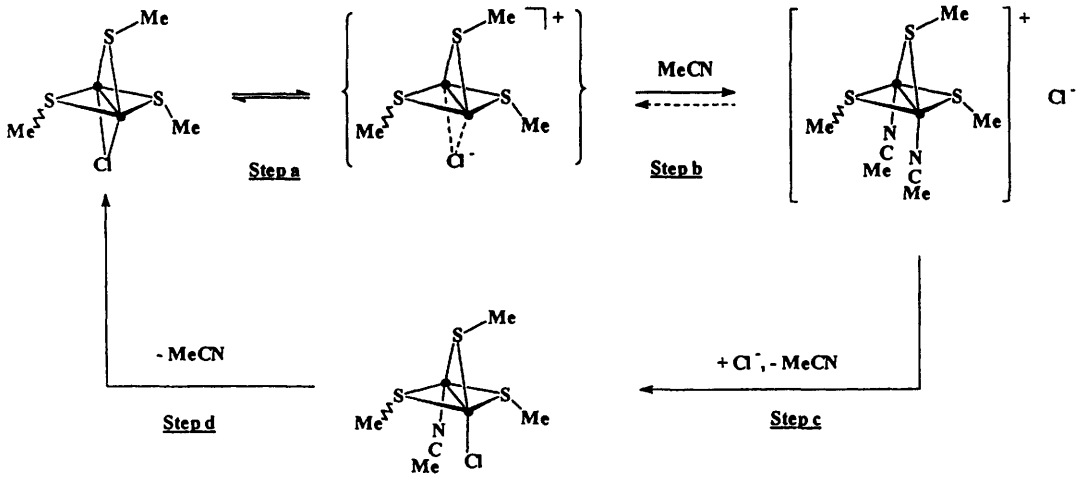

Scheme 4 ● = Mo(cp). Step d is faster than c

to regenerate the parent μ-Cl complex. The attack on chloride ion of the ion pair by H^+ (or by K^+) would shift the equilibrium in step a toward the right-hand side; in addition, the removal of Cl^- as HCl (or as KCl) would prevent regeneration of the starting material from the bis(acetonitrile) cation, and therefore favour the formation of $[Mo_2(cp)_2(\mu\text{-}SMe)_3(MeCN)_2]^+$ in agreement with the experimental results obtained under these conditions. The effect of adding chloride, *e.g.* suppression of the formation of the cation from the chloride-bridged parent, and regeneration of this species from $[Mo_2(cp)_2(\mu\text{-}SMe)_3(MeCN)_2]^+$ and an excess of Cl^-, could be rationalized by the reverse reactions in steps a and b (Scheme 4).

However, an alternative route, which we believe is more likely, is also shown in Scheme 4. The initial attack of Cl^- at a metal centre of the bis(acetonitrile) cation would produce $[Mo_2(cp)_2(\mu\text{-}SMe)_3(\mu\text{-}Cl)]$ *via* the $[Mo_2(cp)_2(\mu\text{-}SMe)_3Cl(MeCN)]$ intermediate and subsequent fast release of MeCN (Scheme 4, steps c and d). The ion $[Mo_2(cp)_2(\mu\text{-}SMe)_3(MeCN)_2]^+$ is the analogue of $[Mo_2(cp)_2(\mu\text{-}SMe)_3(CO)_2]^+$, the electrochemical behaviour of which has been reported previously.[1] The electronic effect of the substitution of the CO groups by MeCN is illustrated by the magnitude of the negative shift of the redox potentials of the complex ($\Delta E^{\ddagger}_{oxl} = 0.9$, $\Delta E_{p_{red}} = 0.7$ V). The electrochemistry and the reactivity of the bis(acetonitrile) cation are currently being explored since substitution of the MeCN ligands could lead to complexes where the substrates are bound to both metal centres.

Conclusion

These results present an original mechanism for the deprotection of a co-ordination site which is interesting in the context of site–substrate interactions and recognition.

(1) In the neutral complex the chloride bridge is locked, as shown by the fact that, in thf, the neutral precursor does not react with CO or isocyanides under the conditions of the electrochemical experiments; the formation of $[Mo_2(cp)_2(\mu\text{-}SMe)_3Cl(Y{\equiv}Z)]$ (Y≡Z = Bu^{t}NC or CO), which are stable complexes, requires an oxidation/reduction sequence. In methyl cyanide $[Mo_2(cp)_2(\mu\text{-}SMe)_3(\mu\text{-}Cl)]$ undergoes a different type of reaction: the chloride bridge is lost in a reaction which is assisted by protons or K^+, and which can be reversed by addition of chloride. The reactivity of the bis(acetonitrile) cation will be explored further since it could be the precursor of complexes where a substrate is co-ordinated to (and possibly activated by) both metal centres.

(2) The one-electron oxidation of the complex unlocks the chloride bridge, but the radical cation retains the quadruply bridged geometry of the neutral parent as shown by EPR spectroscopy and by the fact that the first oxidation system of $[Mo_2(cp)_2(\mu\text{-}SMe)_3(\mu\text{-}Cl)]$ is quasi-reversible in thf and dichloromethane in the absence of a substrate.

(3) The actual opening of the chloride bridge of $[Mo_2(cp)_2(\mu\text{-}SMe)_3(\mu\text{-}Cl)]^{\bullet+}$ is triggered by the substrate.

(4) One of the difficulties we had met in previous studies was that the site, when generated in the absence of substrate, underwent deactivation to stable complexes. In the present case this difficulty is circumvented since the active site possesses a protective device which remains until a potential substrate is present. In addition, when the bound substrate is released, either because of a reversible binding step or following a one-electron reduction, the protective device still operates to prevent decomposition. In our previous studies substrate loss led to deactivation again.[30]

(5) The selectivity of the site is revealed at different levels. The first includes the nature and the rates of the reactions of the different substrates with $[Mo_2(cp)_2(\mu\text{-}SMe)_3(\mu\text{-}Cl)]^{\bullet+}$: we showed that the cyanide ligand reduces the site (still without decomposition of the μ-Cl complex), that CO reacts more slowly than Bu^{t}NC and MeCN, and that MeCN is bound less tightly than CO and Bu^{t}NC. The reduction of the $[Mo_2(cp)_2(\mu\text{-}SMe)_3Cl(Y{\equiv}Z)]^{\bullet+}$ complex displays 'second-order' selectivity: among the substrates studied, only CO and Bu^{t}NC could possibly be reduced by such a complex since the $[Mo_2(cp)_2(\mu\text{-}SMe)_3Cl(Y{\equiv}Z)]$ assembly survives the one-electron reduction only for Y≡Z = CO and Bu^{t}NC. This is illustrated in Scheme 5 (Y≡Z = CO or Bu^{t}NC; Y≡Z* = MeCN).

(6) These results also suggest a competitive inhibition pathway which could switch a substrate reduction process to proton reduction. Both Y≡Z and Y≡Z* (Scheme 5) can bind at the activated site, but Y≡Z* is lost on reduction of [site-Y≡Z*], whereas the [site-Y≡Z] analogue can be reduced without releasing Y≡Z; protonation and further reduction of this species could therefore occur. From Scheme 5 it can be seen that the binding of Y≡Z* would inhibit the reduction of Y≡Z provided they both react at the active site with similar rates [this is not the case for MeCN (Y≡Z*) and Bu^{t}NC or CO (Y≡Z) in the present study]. In the presence of both Y≡Z and Y≡Z* the overall process would be unproductive in terms of substrate reduction since it would only result in proton reduction. On the contrary, in the absence of Y≡Z*, electron transfers could lead to substrate reduction. Such a pathway, based on the different affinity of a competitive inhibitor for two redox states of a single complex, could be relevant to biological processes, provided some modifications are made to the reactions shown in Scheme 5; for example, the nature of the electron-transfer steps might be reversed, with the active site being generated by a reduction step rather than by an oxidation as is the case here.

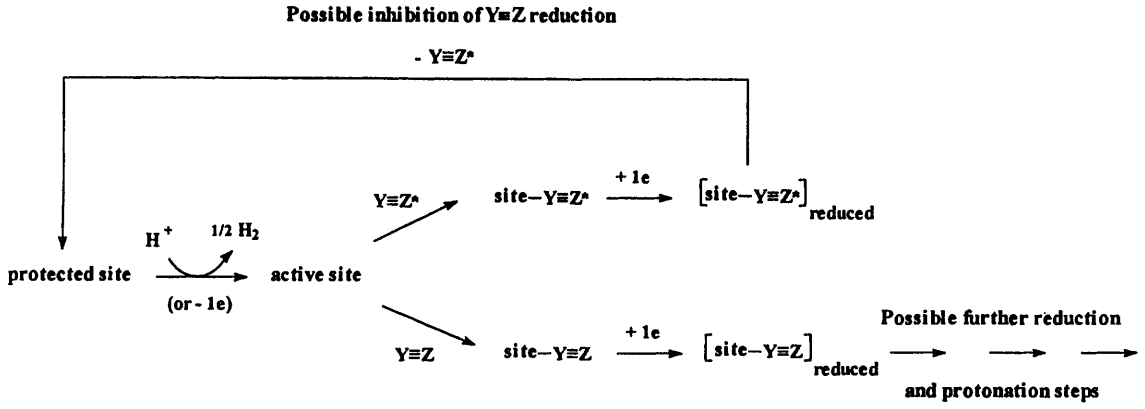

Scheme 5

(7) We think that the reactions described here, that is redox-induced deprotection of a site, ligand binding and possible reprotection of the site, show some similarities with the electron-transfer-induced $\eta^2 \longrightarrow \eta^1$ isomerization of organic ligands.[10–13] Owing to this and because the ligands (CO, RNC, MeCN) are bound terminally to one Mo atom, one may consider that the site is generated at a $Mo(SMe)_3$ centre, which can be viewed as a rudimentary reactivity model of the molybdenum centre in the FeMo cofactor. It is difficult to assess whether or not the second molybdenum centre in the complex plays an active part in the binding step, *i.e.* what exactly is its electronic effect on the reactivity and on selectivity of the site. It is clear that it is directly involved in the protection/deprotection process since one of its obvious roles is to keep the chloride ligand in proximity of the reactive site. This is what an organic hemilabile ligand could also do.[10]

Experimental

Methods and materials

All the experiments were carried out under an inert atmosphere, using Schlenk techniques for the syntheses. Tetrahydrofuran and CH_2Cl_2 were purified as described previously.[1] Acetonitrile (Carlo Erba or BDH, HPLC grade) was used as received. The preparation and purification of the supporting electrolyte $[NBu_4][PF_6]$ were as described previously.[1] Infrared spectra were obtained with a Perkin-Elmer 1430 and ^1H NMR spectra on a Bruker AC300 spectrophotometer. Shifts are relative to tetramethylsilane as internal reference. The EPR spectra were recorded on a JEOL FE 3X apparatus. Chemical analyses were performed by the Centre de Microanalyses du CNRS, Vernaison. The complex $[Mo_2(cp)_2(\mu\text{-}SMe)_3(\mu\text{-}Cl)]$ was prepared as described in the literature.[31]

Electrochemistry

Cyclic voltammetry experiments and controlled-potential electrolyses were performed using Tacussel GCU or PJT 120 potentiostats interfaced with a PAR model 175 waveform generator. The data were recorded on a SEFRAM TGM 164 X-Y recorder. For coulometric experiments, Tacussel IG5N or IG6N electronic integrators were employed. The working electrode used for cyclic voltammetry and amperometric experiments was a Metrohm 628 with a vitreous carbon disc. The secondary electrode was either a carbon rod or a platinum wire. The reference was a $Ag–Ag^+$ electrode. Ferrocene was added as an internal standard at the end of the experiments, and all the potentials given throughout the paper are referred to the ferrocene–ferrocenium couple. The working electrode used for controlled-potential electrolysis and coulometric experiments was a platinum foil.

Kinetic measurements

All kinetic experiments were run under pseudo-first-order conditions at room temperature, using amperometry at a rotating (5000 revolutions min^{-1}) vitreous carbon-disc electrode. The potential of the electrode was set at −0.5 V, that is on the diffusion plateau of the reduction wave of $[Mo_2(cp)_2(\mu\text{-}SMe)_3(\mu\text{-}Cl)]^{\bullet+}$. The intensity of the current and the concentration of $[Mo_2(cp)_2(\mu\text{-}SMe)_3(\mu\text{-}Cl)]^{\bullet+}$ obey the Levich equation $i_l = 0.620nFAD_0^{\frac{2}{3}}\omega^{\frac{1}{2}}\nu^{-\frac{1}{6}}c_t = Bc_t$ (where n is the number of electrons, F is the Faraday constant, A is the electrode area, D_0 is the diffusion coefficient, ω is the rotation speed, ν is the kinematic viscosity and c_t is the complex concentration).

For the experiments with Bu^tNC where the reaction goes to completion the classical equation for a pseudo-first-order reaction, $\ln [c_0/(c_0 - x)] = k't$ where c_0 = initial concentration and $(c_0 - x)$ = concentration at instant t becomes $\ln (i_0/i_t) = k't$, where i_0 is the initial current and i_t that at instant t. The slope of the linear plot $\log (i_0/i_t) = f(t)$ (correlation coefficient 0.998–0.999) allows the pseudo-first-order rate constant to be calculated, slope = $k'/2.303$. Rate constant k' was plotted against different isocyanide concentrations, Fig. 9 (correlation coefficient 0.988).

In the case of the reaction with MeCN an equilibrium is reached. The rate constants for the forward and reverse reactions were calculated in two situations, that is (*i*) when $[Mo_2(cp)_2(\mu\text{-}SMe)_3(\mu\text{-}Cl)]^{\bullet+}$ **A** is initially the only metal complex present in solution, and (*ii*) when **A** and $[Mo_2(cp)_2(\mu\text{-}SMe)_3Cl(MeCN)]^{\bullet+}$ **B** are both present initially; the latter situation results from a second (and subsequent) addition(s) of MeCN to the solution.

Case (*i*). The classical rate law, $\ln [x_{eq}/(x_{eq} - x)] = [c_0k_b/(c_0 - x_{eq})]t$, can be transformed using the expression of the initial current ($i_0 = Bc_0$), of the equilibrium current $[i_{eq} = B(c_0 - x_{eq})]$, and of the current at instant t $[i_t = B(c_0 - x)]$ into $\ln [(i_0 - i_{eq})/(i_t - i_{eq})] = (i_0k_b/i_{eq})t$. The first-order rate constant of the reverse reaction can be calculated from the slope of the linear plot $\log [(i_0 - i_{eq})/(i_t - i_{eq})] = f(t)$, slope = $i_0k_b/2.303i_{eq}$. The pseudo-first-order rate constant, k'_f, was calculated from the equilibrium equation $k'_f = k_bx_{eq}/(c_0 - x_{eq})$, and using the current–concentration relationships, it is defined as $k'_f = k_b(i_0 - i_{eq})/i_{eq}$.

Case (*ii*). This situation, obtained after a first addition of MeCN to a solution of the chloride-bridged radical cation, is illustrated schematically in Fig. 11. The initial current of the second experiment is the same as the equilibrium current of the preceding one, and a new equilibrium is reached after the second addition of MeCN (i_{eq2}). The concentrations of reactant and products are as shown in Scheme 6. Under these conditions, the rate law is given in equation (1). Using the expression of the

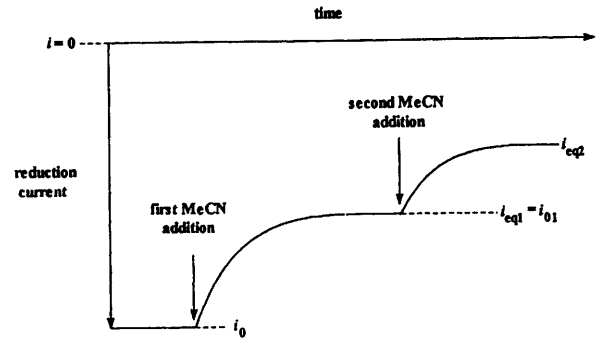

Fig. 11 Schematic representation of the current *vs.* time variation for the amperometric monitoring of the MeCN-binding step. The values of the current intensities used in the calculations are indicated

$$\ln [x_{eq2}/(x_{eq2} - x)] = k_b[(c_{01} + c_{0B})/(c_{01} - x_{eq2})]t \quad (1)$$

initial current ($i_{01} = Bc_{01}$), of the current at instant t [$i_t = B(c_{01} - x)$], and of the equilibrium current [$i_{eq2} = B(c_{01} - x_{eq2})$], and the value of the initial concentration of complex **B** [$c_{0B} = (i_0 - i_{01})/B$], equation (2) can be derived. The first-

$$\ln [(i_{01} - i_{eq2})/(i_t - i_{eq2})] = (i_0 k_b/i_{eq2})t \quad (2)$$

order rate constant of the reverse reaction was calculated from the slope of the linear plot log $[(i_{01} - i_{eq2})/(i_t - i_{eq2})] = f(t)$, slope $= i_0 k_b/2.303 i_{eq2}$. The pseudo-first-order rate constant k'_f was obtained from the equilibrium equation $k'_f = k_b [(c_{0B} + x_{eq2})/(c_{01} - x_{eq2})]$, that is $k'_f = k_b(i_0 - i_{eq2})/i_{eq2}$. A plot of k'_f against five acetonitrile concentrations was linear (correlation coefficient 0.989).

Chemical syntheses

$[Mo_2(cp)_2(\mu\text{-}SMe)_3(\mu\text{-}Cl)]BF_4$. To a solution of $[Mo_2(cp)_2(\mu\text{-}SMe)_3(\mu\text{-}Cl)]$ (0.20 g, 0.4 mmol) in CH_2Cl_2 (20 cm^3) was added 1 equivalent HBF_4–Et_2O. The solution turned instantly from brownish green to purple. Addition of diethyl ether (20 cm^3) precipitated $[Mo_2(cp)_2(\mu\text{-}SMe)_3(\mu\text{-}Cl)]BF_4$ as a purple solid (0.19 g, 80%) (Found: C, 27.2; H, 3.3; Cl, 6.2. Calc. for $C_{13}H_{19}BClF_4Mo_2S_3$: C, 26.7; H, 3.3; Cl, 6.0%).

$[Mo_2(cp)_2(\mu\text{-}SMe)_3Cl(RNC)]BF_4$ (R = Bu^t or $C_6H_3Me_2$). To a solution of $[Mo_2(cp)_2(\mu\text{-}SMe)_3(\mu\text{-}Cl)]BF_4$ (0.23 g, 0.4 mmol) in CH_2Cl_2 (20 cm^3) was added an excess of isocyanide (5 equivalents). The solution was stirred for 20 min at room temperature during which time it turned from purple to dark red. The volume was then reduced under vacuum and ether was added to precipitate the brown product, *ca.* 90% yield (R = Bu^t, 0.24; $C_6H_3Me_2$, 0.25 g). R = Bu^t (Found: C, 31.9; H, 4.0; N, 2.0. Calc. for $C_{18}H_{28}BClF_4Mo_2NS_3$: C, 32.3; H, 4.2; N, 2.1%): IR (CH_2Cl_2) $\tilde{\nu}$(CN)/cm^{-1} 2100s. R = $C_6H_3Me_2$ (Found: C, 35.4; H, 3.8; N, 1.6. Calc. for $C_{22}H_{28}BClF_4Mo_2NS_3$: C, 36.9; H, 3.9; N, 1.9%): IR (CH_2Cl_2) $\tilde{\nu}$(CN)/cm^{-1} 2160s.

$[Mo_2(cp)_2(\mu\text{-}SMe)_3Cl(CO)]BF_4$. A solution of $[Mo_2(cp)_2(\mu\text{-}SMe)_3(\mu\text{-}Cl)]BF_4$ (0.12 g, 0.2 mmol) in CH_2Cl_2 (20 cm^3) was stirred overnight at room temperature under 1 atm CO. Addition of ether precipitated $[Mo_2(cp)_2(\mu\text{-}SMe)_3Cl(CO)]BF_4$ as a brown solid in 90% yield (Found: C, 27.7; H, 3.4. Calc. for $C_{14}H_{19}BClF_4Mo_2OS_3$: C, 27.4; H, 3.1%). IR (CH_2Cl_2): $\tilde{\nu}$(CO)/cm^{-1} 2010s.

The complex $[Mo_2(cp)_2(\mu\text{-}SMe)_3Cl(MeCN)]BF_4$ was prepared *in situ* as described above for the isocyanide and for the carbonyl derivatives. However, it could not be isolated since the acetonitrile ligand is lost when the solution is taken to dryness, and the parent $[Mo_2(cp)_2(\mu\text{-}SMe)_3(\mu\text{-}Cl)]^{+}$ was recovered.

$$\begin{array}{ccccc} & A & + & MeCN & \underset{k_f}{\overset{k_b}{\rightleftharpoons}} & B \\ t = 0 & c_{01} & & \text{excess} & & c_{0B} \\ t & c_{01} - x & & & & c_{0B} + x \\ \text{At equilibrium} & c_{01} - x_{eq2} & & & & c_{0B} + x_{eq2} \end{array}$$

Scheme 6

$[Mo_2(cp)_2(\mu\text{-}SMe)_3(MeCN)_2]BF_4$. To a solution of $[Mo_2(cp)_2(\mu\text{-}SMe)_3(\mu\text{-}Cl)]$ (0.20 g, 0.4 mmol) in MeCN (20 cm^3) was added 1 equivalent of an aqueous HBF_4 solution. The solution turned instantly from brownish green to red. The volume was then reduced under vacuum and ether added to precipitate the complex $[Mo_2(cp)_2(\mu\text{-}SMe)_3(MeCN)_2]BF_4$ as a red solid (yield: 0.23 g, 90%) (Found: C, 31.6; H, 4.0; N, 3.7. Calc. for $C_{17}H_{25}BF_4Mo_2N_2S_3$: C, 32.3; H, 4.0; N, 4.4%). IR (KBr pellet): $\tilde{\nu}$(CN)/cm^{-1} 2250w. ^{1}H NMR (CD_3COCD_3): δ 5.39 (10 H, s, C_5H_5), 2.63 (6 H, s, CH_3CN), 1.96 (3 H, s, SCH_3), 1.92 (3 H, s, SCH_3) and 1.36 (3 H, s, SCH_3).

Acknowledgements

The Centre National de la Recherche Scientifique and the Université de Bretagne Occidentale are acknowledged for financial support. The Ministére de l'Enseignement Supérieur et de la Recherche and the Council of Région Bretagne are acknowledged for providing studentships (to F. B. and S. P.-G.). We are grateful to Dr. F. Conan for recording EPR spectra and for helpful discussions.

References

1 F. Gloaguen, C. Le Floch, F. Y. Pétillon, J. Talarmin, M. El Khalifa and J. Y. Saillard, *Organometallics*, 1991, **10**, 2004.
2 F. Y. Pétillon, S. Poder-Guillou, P. Schollhammer and J. Talarmin, unpublished work.
3 D. S. Tucker, S. Dietz, K. G. Parker, V. Carperos, J. Gabay, B. Noll, M. Rakowski DuBois and C. F. Campana, *Organometallics*, 1995, **14**, 4325.
4 F. Abugideiri, G. A. Brewer, J. U. Desai, J. C. Gordon and R. Poli, *Inorg. Chem.*, 1994, **33**, 3745.
5 J. U. Desai, J. C. Gordon, H.-B. Kraatz, V. T. Lee, B. E. Owens-Waltermire, R. Poli, A. L. Rheingold and C. B. White, *Inorg. Chem.*, 1994, **33**, 3752.
6 J. R. Dilworth, B. D. Neaves, C. J. Pickett, J. Chatt and J. A. Zubieta, *Inorg. Chem.*, 1983, **22**, 3524.
7 T. I. Al Salih and C. J. Pickett, *J. Chem. Soc., Dalton Trans.*, 1985, 1255.
8 S. K. Ibrahim and C. J. Pickett, *J. Chem. Soc., Chem. Commun.*, 1991, 246.
9 C. Amatore, S. Aziz, A. Jutand, G. Meyer and P. Cocolios, *New J. Chem.*, 1995, **19**, 1047.
10 D. L. Hughes, S. K. Ibrahim, C. J. Pickett, G. Querné, A. Laouénan, J. Talarmin, A. Queiros and A. Fonseca, *Polyhedron*, 1994, **13**, 3341.
11 W. D. Harman, M. Sekine and H. Taube, *J. Am. Chem. Soc.*, 1988, **110**, 2439.
12 D. W. Powell and P. A. Lay, *Inorg. Chem.*, 1992, **31**, 3542.
13 C. A. Sassano and C. A. Mirkin, *J. Am. Chem. Soc.*, 1995, **117**, 11379.
14 N. G. Connelly and L. F. Dahl, *J. Am. Chem. Soc.*, 1970, **92**, 7470.
15 A. J. Bard and L. R. Faulkner, *Electrochemical Methods. Fundamentals and Applications*, Wiley, New York, 1980, ch. 11, pp. 429–485; E. R. Brown and R. F. Large, in *Techniques of Chemistry*, ed. A. Weissberger, Wiley, New York, 1971, vol. 1, Part IIA, ch. 6, pp. 423–530.
16 J. C. Gaudiello, T. C. Wright, R. A. Jones and A. J. Bard, *J. Am. Chem. Soc.*, 1985, **107**, 888; A. Fitch and G. J. Edens, *J. Electroanal. Chem. Interfacial Electrochem.*, 1989, **267**, 1.
17 J. Chatt, C. T. Kan, G. J. Leigh, C. J. Pickett and D. R. Stanley, *J. Chem. Soc., Dalton Trans.*, 1980, 2032.
18 A. J. L. Pombeiro, C. J. Pickett and R. L. Richards, *J. Organomet. Chem.*, 1982, **224**, 285.
19 C. J. Casewit and M. Rakowski DuBois, *Inorg. Chem.*, 1986, **25**, 74.
20 R. E. Dessy, R. Kornmann, C. Smith and R. Haytor, *J. Am. Chem. Soc.*, 1968, **90**, 2001.

21 M. B. Robin and P. Day, *Adv. Inorg. Chem. Radiochem.*, 1967, **10**, 700.
22 J. C. Green, M. L. H. Green, P. Mountford and M. J. Parkington, *J. Chem. Soc., Dalton Trans.*, 1990, 3407.
23 D. L. DuBois, W. K. Miller and M. Rakowski DuBois, *J. Am. Chem. Soc.*, 1981, **103**, 3429.
24 W. Tremel, R. Hoffmann and E. D. Jemmis, *Inorg. Chem.*, 1989, **28**, 1213.
25 F. Barrière, F. Y. Pétillon, P. Schollhammer and J. Talarmin, unpublished work.
26 F. Abugideiri, J. C. Fettinger and R. Poli, *Inorg. Chim. Acta*, 1995, **229**, 445.
27 M. L. Abasq, F. Y. Pétillon and J. Talarmin, *J. Chem. Soc., Chem. Commun.*, 1994, 2191.
28 J. Chatt, G. J. Leigh, H. Neukomm, C. J. Pickett and D. R. Stanley, *J. Chem. Soc., Dalton Trans.*, 1980, 121.
29 P. Bernatis, R. C. Haltiwanger and M. Rakowski DuBois, *Organometallics*, 1992, **11**, 2435.
30 M. Guéguen, F. Y. Pétillon and J. Talarmin, *Organometallics*, 1989, **8**, 148.
31 M. B. Gomes de Lima, J. E. Guerchais, R. Mercier and F. Y. Pétillon, *Organometallics*, 1986, **5**, 1952.

Received 4*th March* 1996; *Paper* 6/01505K